




Article

Antioxidant Effects, Antiproliferative Effects, and Molecular Docking of *Clinacanthus nutans* Leaf Extracts

Noor Zafirah Ismail , Zaleha Md Toha, Musthahimah Muhamad, Nik Nur Syazni Nik Mohamed Kamal , Nur Nadhirah Mohamad Zain and Hasni Arsad * 

Advanced Medical and Dental Institute, Universiti Sains Malaysia, Bertam, Kepala Batas 13200, Penang, Malaysia; piecesnzi@gmail.com (N.Z.I.); Zaleha.mdtoha@usm.my (Z.M.T.); musthahimahmuhamad@gmail.com (M.M.); niksyazni@usm.my (N.N.S.N.M.K.); nurnadhirah@usm.my (N.N.M.Z.)

* Correspondence: hasniarsad@usm.my; Tel.: +60-4562-2415

Academic Editors: Luisa Tesoriere and Alessandro Attanzio

Received: 5 February 2020; Accepted: 13 March 2020; Published: 29 April 2020



Abstract: *Clinacanthus nutans* is a well-known herb that has been used as an alternative and therapeutic medicine, however more selective *C. nutans* extracts are needed. In this study, leaves were extracted with 80% methanol and further fractionated with *n*-hexane, dichloromethane, chloroform, *n*-butanol, and aqueous residue. Subsequently, the total phenolic content (TPC), total flavonoid content (TFC), antioxidant scavenging activity, and antiproliferative effects on breast cancer (Michigan Cancer Foundation-7 [MCF7]) and normal breast (Michigan Cancer Foundation-10A [MCF 10A]) cells of the extracts were measured. Additionally, molecular docking simulation of the major compounds from *C. nutans* extracts was conducted. The aqueous residue had the highest TPC and TFC, whereas the crude extract had the highest scavenging activity. Among the extracts, dichloromethane extract (CN-Dcm) was selected as it had the highest selectivity index (SI) (1.48). Then, the chosen extract (CN-Dcm) was proceed for further analysis. The compounds from CN-Dcm were identified using gas chromatography–mass spectrometry (GC-MS). The major compounds from CN-Dcm were further investigated through molecular docking studies. Palmitic acid and linolenyl alcohol were the compounds found in the CN-Dcm extract that exhibited the highest binding affinities with p53-binding protein Mdm-2. These results highlight the potential of *C. nutans* as a source of anticancer activities.

Keywords: *Clinacanthus nutans*; antiproliferative effect; antioxidant; GC-MS; molecular docking

1. Introduction

Cancer is a major health problem and the most devastating life-threatening disease worldwide [1]. It is characterized by dysregulated cell growth, cell division, and cell death, and by the rapid proliferation of abnormal cells [2]. Global Cancer Incidence, Mortality and Prevalence (GLOBOCAN) reported that from 2012, 1.67 million new breast cancer cases occurred worldwide [3], and breast cancer is the most common cancer among Malaysian women [4]. Although the majority of breast cancer patients are female, a small number of men also suffer from breast cancer [4]. To date, chemotherapy is the first therapeutic strategy to fight cancers, despite the strong side effects. [5]. Natural products can assist the action of chemotherapy but cannot replace them yet. The demand for natural products, especially from medicinal plants, has increased because chemotherapeutic drugs are expensive, lead to morbidity, and have many side effects [6].

Clinacanthus nutans is a medicinal plant that has many medicinal properties, including treating lesions generated by the herpes-simplex virus, antiinflammatory, anticancer, antibacterial, and

antivenom activities [7]. *C. nutans* is found in Malaysia, Vietnam, Indonesia, Thailand, and China [8,9], and occurs in most habitats [10]. Many studies carried out abroad have proven the effectiveness of *C. nutans* as an anticancer agent on several types of cancer cells. However, there is still lack of information on the effectiveness of *C. nutans* fraction solvent from various degrees of polarity on breast cancer cells. Michigan Cancer Foundation-7 (MCF7) is the favored cell line, mainly because of its sensitivity to the hormone estrogen, as it possesses estrogen receptors [11]. MCF7 is an ideal model for an in vitro hormone response study because it works well when incorporated into xenograft models, such as rabbit or mice models for in vivo tumorigenic experiments in the presence of estrogen, compared to breast cancer cell lines, such as MDA-MB-453 and SKBR3 cells, which do not have significant in vivo tumorigenic potential [12], or MDA-MB-231, which has poor in vivo metastatic effects [13]. Additionally, some MCF7 in vitro therapeutic response research studies have been translated to successful clinical trials and subsequent development of anticancer drugs [14].

Therefore, this study would be beneficial to further explore the antiproliferative effect of *C. nutans* extract on MCF7 cells. Additionally, many *C. nutans* studies did not evaluate the effect of *C. nutans* extracts on normal breast cancer cells. The use of normal cells ensures that the *C. nutans* extracts are not toxic to healthy cells. Thus, the goal of this study was to test the ability of different extracts of *C. nutans* to inhibit breast cancer cell proliferation. We measured the total phenolic content (TPC), total flavonoid content (TFC), and antioxidant scavenging activity of the *C. nutans* crude extract and its fractions using 2,2-diphenyl-1-picrylhydrazyl (DPPH) and 2,2'-azino-bis(3-ethylbenzothiazoline-6-sulfonic acid (ABTS) assays. We also evaluated the effects of the extracts on the cell growth of estrogen responsive breast cancer (MCF7) and normal breast (MCF 10A) cells, identified compounds from selected extracts using gas chromatography–mass spectrometry (GC-MS), and investigated the major compounds using molecular docking studies to evaluate their binding affinities with targeted apoptosis proteins.

2. Results and Discussion

2.1. Extraction Yield

Extraction of *C. nutans* leaves was performed using 80% methanol. The crude methanolic extract was further fractionated sequentially with different solvents (hexane, dichloromethane, chloroform, *n*-butanol, and aqueous residue). The effectiveness of plant extraction depends on the extraction method and on the solvent used, as solvents with different polarities have a significant effect on the chemical contents of the extracts. Thus, it is important to identify the optimal solvents for extraction of antioxidant compounds from medicinal plants [15]. Water was employed for the extraction because of its universal solubility of polar compounds, while methanol was chosen due to its ability to extract lower molecular weight polyphenols [16] and its tendency to yield relevant antioxidant and cytotoxic compounds from *C. nutans* [17]. Part of the crude methanolic extract was fractionated using different solvents to concentrate and enhance the purity of active compounds and remove unwanted interferences [16]. Table 1 shows the percentage yield of crude and fraction extracts of *C. nutans* leaves. The yield of the crude methanolic extract of *C. nutans* leaves (CN-Crd) was 6.85%, and the yield of the fractions varied from 2.18% to 37.71% in the following ascending order: aqueous residue (CN-Aqu) > *n*-butanol (CN-But) > dichloromethane (CN-Dcm) > *n*-hexane (CN-Hex) > chloroform (CN-Chl). The percentage yields were significantly different ($p < 0.05$).

Table 1. Percentage yield of crude and fraction extracts of *C. nutans* leaves.

Type of Extracts	Percentage Yield (%)
CN-Crd	6.85 ± 0.15 ^a
CN-Hex	4.10 ± 0.08 ^b
CN-Dcm	13.73 ± 0.05 ^c
CN-Chl	2.18 ± 0.24 ^d
CN-But	20.16 ± 0.34 ^e
CN-Aqu	37.71 ± 0.09 ^f

Effect of different solvents on extraction yield. The percentage yield shows significantly different ($p < 0.05$). Different lowercase characters represent significant difference ($p < 0.05$). CN-Crd, crude methanolic extract; CN-Hex, hexane fraction extract; CN-Dcm, dichloromethane fraction extract; CN-Chl, chloroform fraction extract; CN-But, *n*-butanol fraction extract; CN-Aqu, aqueous residue fraction extract.

2.2. TPC and TFC

The phenolic and flavonoid contents of the *C. nutans* extracts were measured because they are major contributors to the extract's overall antioxidant activities. Figure 1 shows the TPC and TFC of the *C. nutans* extracts and fractions. The CN-Aqu fraction extract (415.76 mg gallic acid equivalent (GAE)/g extract) contained the highest amount of phenolics and the CN-Hex extract (50.24 mg GAE/g extract) contained the least. TPC values in descending order were as follows: CN-Aqu > CN-But > CN-Dcm > CN-Crd > CN-Chl > CN-Hex. The TPC of the CN-Aqu fraction was higher than other values reported in the literature for *C. nutans* extracts. For example, Sarega et al. [18] reported that the aqueous extract of *C. nutans* had a phenolic content of 63.77 ± 7.31 mg GAE/g extract. On the other hand, other plants reportedly have higher phenolic contents in the *n*-butanol extract, which agreed with the results of this study (i.e., CN-But had the second highest TPC). For instance, the phenolic content of the *n*-butanol extract of *Vernonia blumeoides* was 410 ± 0.8 mg GAE/g extract [19]. In our study, *n*-hexane extract of *C. nutans* had the lowest TPC; similarly, Johari et al. [20] reported that the hexane extract of *Pereskia bleo* had the lowest total phenolic content of 25.20 ± 0.01 mg GAE/g extract. The results of our analysis showed that TFC was lower than TPC in all extracts. This was not surprising, as flavonoids are subgroups of phenolics that contribute to the overall amounts of phenolics [20].

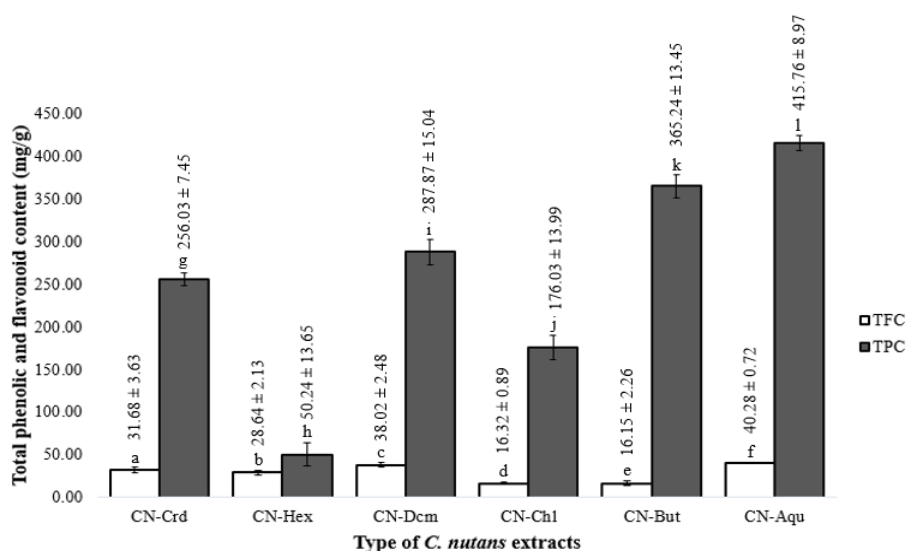


Figure 1. Total phenolic contents (TPC) and total flavonoid contents (TFC) of crude and fraction of *C. nutans* leaf extracts. A comparison of TPC and TFC in different *C. nutans* extracts; data represent mean ± SD, $n = 3$. LSD, least significant difference; level of significance: $p < 0.05$ using Bonferroni test analysis. Different lowercase characters represent significant difference.

2.3. Antioxidant Capacities

The antioxidant capacities of the *C. nutans* extracts were quantified using 2,2-diphenyl-1-picrylhydrazyl (DPPH) and 2,2'-azino-bis(3-ethylbenzothiazoline-6-sulfonic acid (ABTS) assays. The use of at least two methods is recommended to evaluate and compare the antioxidant capacity of a sample [21]. Because they are stable radicals, DPPH and ABTS are widely used to determine the antioxidant activity of plants [22,23]. Table 2 shows the half-maximal effective concentration (EC₅₀) of the extracts and fractions of *C. nutans* leaves. The EC₅₀ is the concentration of antioxidant that causes a 50% decrease in radical absorbance, which is commonly assessed by measuring antioxidant concentration readings [24]. Trolox, which is a well-known natural antioxidant, was used as the standard. The *C. nutans* extracts ranged between 125 and 4000 µg/mL. The antioxidant activities measured using the ABTS assay were lower than values determined by the DPPH assay, which is in agreement with results reported by Lachman et al. [25]. Samples with lower EC₅₀ values are considered to have high antioxidant capacity [26]. The EC₅₀ values calculated from the DPPH and ABTS assays for the crude and fraction extracts of *C. nutans* ranged from 560.50 to 1530.00 µg/mL and from 476.30 to 1024.00 µg/mL, respectively. Based on the EC₅₀ value, CN-Hex had the lowest antioxidant activity and CN-Crd had the highest antioxidant activity. Haron et al. [17] also reported that the crude methanol extract of *C. nutans* leaves showed the highest scavenging effect (DPPH = 21.18 mg Trolox/g, ABTS = 11.80 mg Trolox/g), while the hexane fraction had the lowest scavenging activity (DPPH = 1.06 mg Trolox/g). However, Alam et al. [27] reported that the crude methanol extract of *C. nutans* leaves had the lowest scavenging activity. These differences in results likely occurred because the plants are largely influenced by environmental conditions, such as temperature, rainfall, water variability, humidity, variations in soil pH, nutrient contents, and exposure to soil microorganisms [28]. Moreover, environmental factors interact with the genetics of the plants, which lead to genetic variations [29] that affect the phytochemical contents.

Table 2. The half-maximal effective concentration (EC₅₀) of *C. nutans* crude and fraction extracts for 2,2-diphenyl-1-picrylhydrazyl (DPPH) and 2,2'-azino-bis(3-ethylbenzothiazoline-6-sulfonic acid (ABTS) radical scavenging activities.

Type of Extracts	DPPH (µg/mL)	ABTS (µg/mL)
CN-Crd	560.50 ± 2.45	476.30 ± 0.74
CN-Hex	1530.00 ± 3.74	1024.00 ± 4.18
CN-Dcm	1039.00 ± 0.87	937.00 ± 3.84
CN-Chl	796.40 ± 7.21	602.50 ± 1.74
CN-But	837.10 ± 3.14	837.40 ± 9.45
CN-Aqu	744.30 ± 8.45	718.00 ± 1.84
Trolox standard	32.33 ± 2.47	37.74 ± 2.15

Effect of EC₅₀ of *C. nutans* crude and fraction extracts. The EC₅₀ are significantly different ($p < 0.05$). CN-Crd, crude methanolic extract; CN-Hex, hexane fraction extract; CN-Dcm, dichloromethane fraction extract; CN-Chl, chloroform fraction extract; CN-But, *n*-butanol fraction extract; CN-Aqu, aqueous residue fraction extract.

2.4. Antiproliferative Assay

The antiproliferative activity of the extracts was assessed using the sulforhodamine B (SRB) assay. SRB is a fluorescent dye used to quantify the proteins present in cultured cells. The SRB dye binds to the amino acids of cellular proteins and then the dye can be used to estimate the cell viability [30]. Based on the SRB assay, we compared the results of the SRB assay with 3-(4,5-dimethylthiazol-2-yl)-5-(3-carboxymethoxyphenyl)-2-(4-sulfophenyl)-2H-tetrazolium (MTS) and alamar blue assays at 72 h of exposure (Table S1). The results showed no significant differences between three cytotoxicity assays ($p > 0.05$), which were in agreement with studies reported by Aslantürk [31] and Vajrabhaya and Korsuwannawong [32]. The 3-(4,5-dimethylthiazol-2-yl)-2,5-diphenyl-2H-tetrazolium bromide (MTT) assay was a commonly used cytotoxicity assay. However, van Tonder et al. [33] describes that the MTT assay was less accurate in detecting changes in cell numbers. They [33] also

expressed that that SRB assay appears to be more sensitive than MTT assay, which was in line with the studies by Skehan et al. [34] and Vajrabhaya and Korsuwannawong [32], who reported that SRB assay had better linearity with cell number and higher reproducibility. Thus, we choose SRB assay to report the antiproliferative effects of crude and fraction extracts of *C. nutans*.

The antiproliferative activities of the crude and fraction extracts of *C. nutans* leaves were tested on MCF7 and MCF 10A cells to determine their inhibitory effects on cell proliferation. Figure 2 shows the effect of various concentrations of crude and fraction extracts on cell viability of MCF7 and MCF 10A cells. Tamoxifen was used as the positive control and its IC₅₀ for MCF7 cells was 3.42 ± 0.46 µg/mL. Tamoxifen also inhibited MCF 10A normal breast cells, with an IC₅₀ value of 1.67 ± 0.31 µg/mL. The CN-Crd extract inhibited 50% of MCF7 cell growth at 496.50 ± 0.45 µg/mL. This result is in agreement with the observed cytotoxic effect of the crude methanol extract of *C. nutans* leaves on human immortalized myelogenous leukemia (K-562) cells, with IC₅₀ >100 µg/mL at 72 h [35]. Our results showed that CN-Crd had a low inhibitory effect on MCF7 cells. Haron et al. [36] also showed that the crude extract had a low inhibitory effect on cervical cancer (HeLa) cells. Based on the antiproliferative activity of MCF10A, the results demonstrated that CN-Crd of *C. nutans* leaves inhibited the growth of MCF 10A cells, with an IC₅₀ of 53.15 ± 0.23 µg/mL.

The CN-Crd extract was sequentially fractionated using *n*-hexane, dichloromethane, chloroform, and *n*-butanol, and the antiproliferative effects of these fractions on MCF7 cells were investigated. Fractionation was performed because fractions of crude alcoholic extracts may have high inhibitory effects against cancer cells [36,37]. Adebayo et al. [37] found that the hexane fraction of the crude 80% ethanolic extract of *Moringa oleifera* had stronger antiproliferation activity against cancer cells compared to the crude extract. Similarly, hexane, dichloromethane, ethyl acetate, and butanol fractions of the crude methanolic extract of *Ziziphus mauritiana* bark had high inhibitory effects on MCF7, HeLa, prostate cancer (PC3), and lung cancer (NCI-H460) cells [38].

In our study, the CN-Hex fraction had the greatest inhibitory effects on MCF7 cells, with an IC₅₀ of 50.34 ± 0.11 µg/mL, followed by the CN-Dcm fraction (IC₅₀ = 65.95 ± 0.17 µg/mL), CN-Chl (IC₅₀ = 67.52 ± 0.17 µg/mL), CN-But (IC₅₀ = 111.50 ± 0.20 µg/mL), and CN-Aqu (IC₅₀ = 398.00 ± 0.24 µg/mL). Wang et al. [39] reported that the IC₅₀ of the hexane fraction of *C. nutans* leaves was 84.77 ± 3.43 µg/mL, which was higher than the IC₅₀ for CN-Hex; this means that the CN-Hex fraction was more toxic than the hexane fraction in Wang et al.'s study [39]. There are no published reports about the antiproliferative effects of the dichloromethane, chloroform, and *n*-butanol fractions of the crude methanolic extract of *C. nutans* on MCF7 cells. However, the inhibitory effect of the CN-Dcm fraction on the growth of MCF7 cells in our study was comparable to the observed antiproliferative effect of the dichloromethane fraction of *C. nutans* leaves on HeLa cells that was reported by Haron et al. [36]. CN-Dcm was more effective for MCF7 cells because it had a lower IC₅₀. On the other hand, CN-Chl inhibited MCF7 cell growth at a lower concentration (67.52 ± 0.17 µg/mL). There was no inhibition of MCF7 cell growth when the cells were treated with CN-Crd and CN-Aqu extracts at concentrations below 100 µg/mL.

The fraction extracts were also tested for their effects on MCF 10A cells (Figure 2b). MCF 10A cells were used to obtain the selective indices (SI) of the extracts. The SI value was calculated as the ratio of the IC₅₀ values of the extracts on MCF 10A cells relative to those in the MCF7 cells. According to Segun et al. [40], an SI value > 1 one suggests that an extract is less toxic to normal cells compared with cancer cells, thus compounds with high SI values can be assumed to offer potential safer therapy. Table 3 shows the SI values of the crude and fraction extracts of *C. nutans* leaves. In ascending order, the SI values were as follows: CN-Dcm > CN-Chl > CN-Hex > CN-But > CN-Aqu > CN-Crd. CN-Dcm inhibited MCF 10A cell growth, with an IC₅₀ value of 100.20 ± 2.88 µg/mL and an SI value of 1.48, which means that this fraction extract was selective. On the other hand, CN-Hex, CN-Chl, CN-Aqu, and CN-Crd inhibited MCF 10A cell growth with IC₅₀ values of 40.43 ± 1.70 µg/mL, 57.55 ± 0.38 µg/mL, 160.40 ± 0.52 µg/mL, and 53.15 ± 0.23 µg/mL, respectively, and had lower SI values than the CN-Dcm fraction. These results suggest that these fractions were more toxic to the normal cells than to the cancer cells. The growth of MCF 10A cells exposed to CN-But was inhibited at an IC₅₀ value of

$86.50 \pm 1.06 \mu\text{g/mL}$, whereas it inhibited the growth of MCF7 cancer cells with an IC_{50} value of $111.50 \pm 0.20 \mu\text{g/mL}$. Thus, the CN-But fraction had selective toxicity to the cancer cells, unlike CN-Hex, CN-Chl, CN-Aqu, and CN-Crd, which non-selectively inhibited the proliferation of both MCF7 and MCF 10A cells.

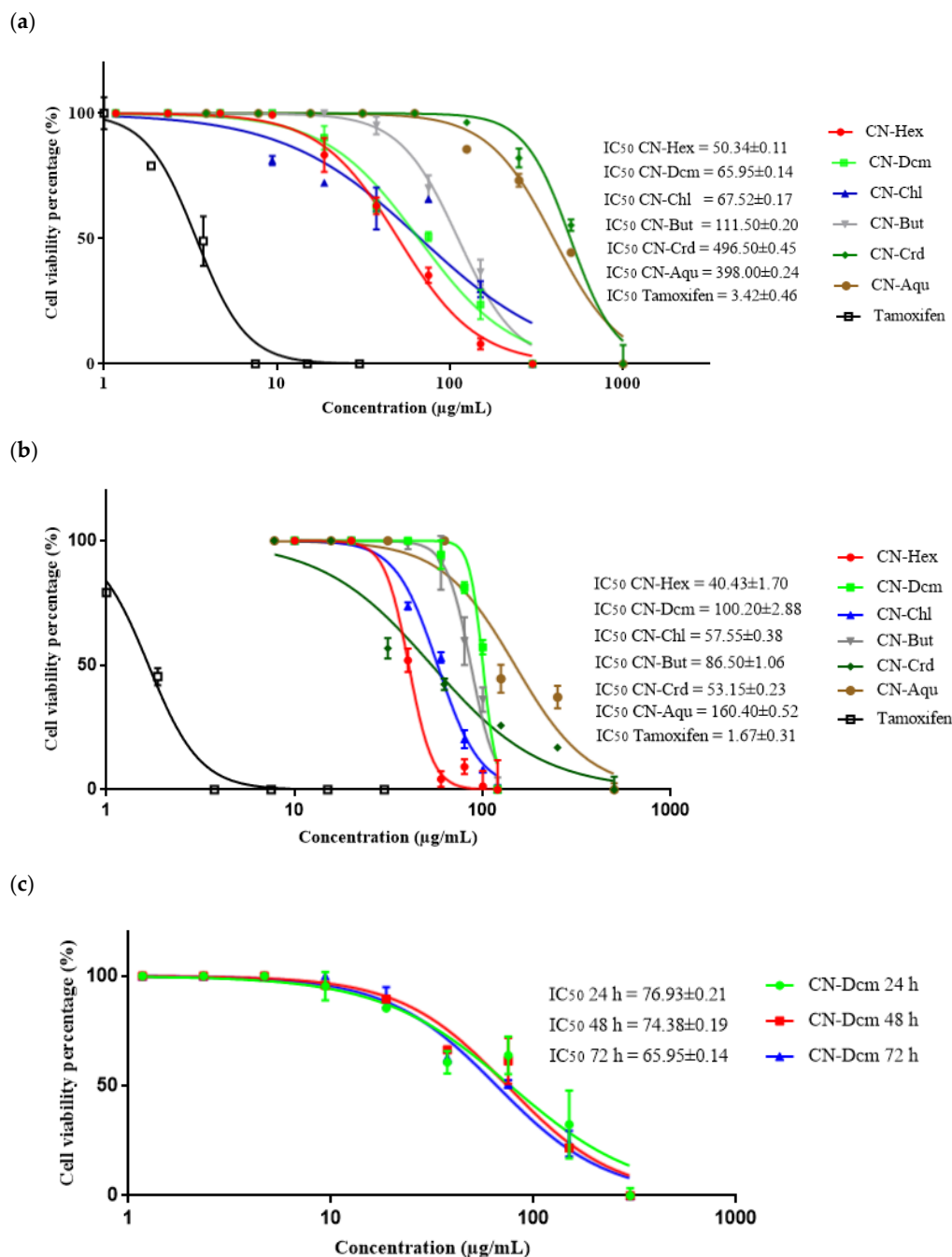


Figure 2. Preliminary screening of the IC_{50} of *C. nutans* crude and fraction extracts using the sulforhodamine B (SRB) assay: (a) antiproliferative effect of *C. nutans* extracts on MCF7 cell viability; (b) antiproliferative effect of *C. nutans* extracts on MCF 10A cells; (c) antiproliferative of the CN-Dcm fraction extract on MCF7 cells at 24, 48, and 72 h of exposure. Results are presented as mean \pm standard deviation (SD) ($n = 3$). CN-Crd, crude methanolic extract; CN-Hex, hexane fraction extract; CN-Dcm, dichloromethane fraction extract; CN-Chl, chloroform fraction extract; CN-But, *n*-butanol fraction extract; CN-Aqu, aqueous residue fraction extract.

Table 3. Selective index of crude and fraction extracts of *C. nutans* leaf activities.

Selective Index	MCF 10A/MCF7
CN-Crd	0.11
CN-Hex	0.80
CN-Dcm	1.48
CN-Chl	0.85
CN-But	0.78
CN-Aqu	0.4
Tamoxifen	0.49

CN-Crd, crude methanolic extract; CN-Hex, hexane fraction extract; CN-Dcm, dichloromethane fraction extract; CN-Chl, chloroform fraction extract; CN-But, *n*-butanol fraction extract; CN-Aqu, aqueous residue fraction extract.

Based on these results, CN-Dcm was the most selective fraction, as it selectively inhibited MCF7 cells and was less toxic to MCF 10A cells. Therefore, it was selected for further investigation. The results were in agreement with previous *C. nutans* studies, in which non-polar to semipolar extracts had higher antiproliferative activity than polar extracts [35,41–43]. However, none of the crude and fraction extracts of *C. nutans* leaves followed the criteria of the National Cancer Institute, which requires a crude plant extract to have an $IC_{50} < 30 \mu\text{g/mL}$ for preliminary assay [44]. The cell viability assay was repeated using the CN-Dcm fraction extract for different incubation times (24, 48, and 72 h). The IC_{50} values for the three time points were plotted (Figure 2c) and show that at 24 h of treatment, CN-Dcm inhibited 50% of cell proliferation at a concentration of $76.93 \pm 0.21 \mu\text{g/mL}$, while at 48 h the IC_{50} of the extract was $74.38 \pm 0.19 \mu\text{g/mL}$ and at 72 h it was $65.95 \pm 0.14 \mu\text{g/mL}$. Thus, the inhibitory activity of this extract occurred in a dose- and time-dependent manner. The IC_{50} of the CN-Dcm fraction decreased when the period of incubation increased.

2.5. GC-MS Spectral Analysis of Compounds Presents in CN-Dcm

We were able to separate and identify various constituents of CN-Dcm using GC-MS analysis. Table 4 summarizes the 14 components identified in the CN-Dcm fraction with their molecular formula, peak percentage, and similarity index. Compounds were identified by referring to the corresponding compound in the National Institute of Standards and Technology (NIST) library; a similarity index of at least 80% was required for identification. The GC-MS analysis revealed the presence of two major components: linolenyl alcohol (29.10%) and palmitic acid (23.84%).

Table 4. Results of the GC-MS analysis of the CN-Dcm fraction of the extract.

Peak	Compound	Retention Time	Molecular Formula	Similarity Index	Peak Percentage (%)
1	Methyl beta-D-glucopyranoside	9.028	C ₇ H ₁₄ O ₆	90	0.97
2	Methyl 4-hydroxycinnamate	9.514	C ₁₀ H ₁₀ O ₃	91	3.81
3	Methyl trans-3-hydroxycinnamate	10.077	C ₁₀ H ₁₀ O ₃	94	11.37
4	Methyl palmitate	10.96	C ₁₇ H ₃₄ O ₂	99	1.55
5	Palmitic acid	11.133	C ₁₆ H ₃₂ O ₂	99	23.84
6	10,13-Octadecadienoic acid, methyl ester	11.807	C ₁₉ H ₃₄ O ₂	99	0.92
7	Methyl linolenate	11.842	C ₁₉ H ₃₂ O ₂	99	5.86
8	Phytol	11.891	C ₂₀ H ₄₀ O	80	0.60
9	Methyl stearate	11.926	C ₁₉ H ₃₈ O ₂	99	0.53
10	Linolenyl alcohol	12.023	C ₁₈ H ₃₂ O	95	29.10
11	Octadecanoic acid	12.078	C ₁₈ H ₃₆ O ₂	99	6.15
12	2-(((2-Ethylhexyl)oxy)carbonyl)benzoic acid	14.045	C ₁₆ H ₂₂ O ₄	91	14.51
13	Glyceryl 2-linolenate	15.053	C ₂₁ H ₃₆ O ₄	99	0.44
14	Oleamide	15.706	C ₁₈ H ₃₅ NO	90	0.34

2.6. Molecular Docking

2.6.1. Drug-Likeness and Toxicity Prediction

The two major compounds found in the CN-Dcm fraction, palmitic acid and linolenyl alcohol (Figure 3), were subjected to drug-likeness and toxicity prediction using Lipinski's rule of five; this rule determines the consistency of orally active drugs [45]. Lipinski's rule of five [45] states that a drug molecule generally does not violate more than one of the following five rules: molecular mass < 500 Da, high lipophilicity (expressed as LogP < than 5), < 5 hydrogen bond donors, < 10 hydrogen bond acceptors, and molar refractivity between 40 and 130 [46,47]. As displayed in Table 5, linolenyl alcohol and palmitic acid did not violate any rules, suggesting that they could be suitable for oral administration.

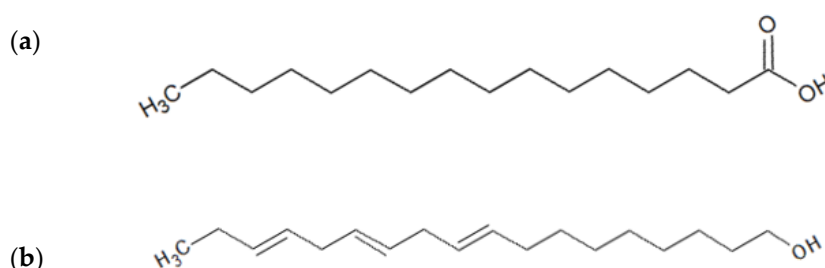


Figure 3. The major compounds found in CN-Dcm fraction extract of *C. nutans* leaves: (a) palmitic acid; (b) linolenyl alcohol.

Table 5. Lipinski's rule for major compounds of CN-Dcm, assessed by SwissADME web tool.

Compound	Molecular Weight (Da)	Hydrogen Bond Donor	Hydrogen Bond Acceptor	LogP	Molar Refractivity	Rules Satisfied
Palmitic acid	256.42	1	2	4.19	80.80	5/5
Linolenyl alcohol	264.45	1	1	4.59	88.38	5/5

2.6.2. Molecular Docking Analysis

Molecular docking analysis is widely used in drug discovery to understand the drug–receptor interaction and gene pathway [48]. The antiproliferative effect of the *C. nutans* extracts may be caused by activation of apoptosis proteins. Apoptosis, or programmed cell death, is an important component of regulation of cell growth and maintenance of tissue homeostasis, and it is restricted during uncontrolled growth of damaged cells [49]. Apoptosis is also the hallmark of cancer [50]. In this analysis, we studied the following apoptosis-related proteins: tumor necrosis factor- α (TNF- α), p53-binding protein Mdm-2, and caspase-3. The p53 tumor suppressor protein activates transcription of proapoptotic genes that encode members of the Bcl-2 family, as well as TNF-related apoptosis [51]. Activation of p53 only occurs through its dissociation from its inhibitor, MDM2; thus, MDM2 inhibitors are considered to be proapoptotic agents [52,53]. Álvarez et al. [54] reported that the cytokine TNF- α can promote activation of caspase-3 by expressing Fas ligand (FasL) through nuclear factor of activated T-cells (NFAT) activation in neuroblastoma cells. Caspase-3 is an essential marker that has been shown to be an entry point in the apoptotic signalling pathway. Hence, caspase-3 is important for the formation of apoptotic bodies and dismantling of the cells, and may function before or after the loss of cell viability [55].

In this study, the proteins TNF- α , p53 binding protein Mdm-2, and caspase-3 were docked with palmitic acid and linolenyl alcohol. Table 6 shows the best result for each compound and the apoptosis proteins. Palmitic acid and linolenyl alcohol had the highest binding affinities towards p53-binding protein Mdm-2, with binding energy values of -4.22 kcal/mol and -4.56 kcal/mol, respectively. According to Pantzar and Poso [56], the lowest binding energies of ligands towards the targeted

proteins result in the highest binding affinities. The lowest binding affinities detected were -2.45 kcal/mol and -2.99 kcal/mol for palmitic acid and linolenyl alcohol with TNF- α protein, respectively.

Table 6. Binding energy of major compounds and apoptosis proteins. TNF- α , tumor necrosis factor- α .

Proteins	Binding Energy (kcal/mol)	
	Palmitic Acid	Linolenyl Alcohol
TNF- α	-2.45	-2.99
p53-binding protein Mdm-2	-4.22	-4.56
Caspase-3	-3.56	-3.93

Protein docking analysis showed that linolenyl alcohol had better binding affinity towards p53-binding protein Mdm-2 compared to palmitic acid. Figure 4 shows results of the interaction pattern analysis of the compounds with apoptosis proteins. Based on the result from Discovery Studio Visualizer 4.1 client, the molecular interactions of linolenyl alcohol with p53-binding protein Mdm-2 formed two Pi-Alkyl interactions with Phe-55 and Tyr-56, two hydrogen bonds were formed, and two hydrophobic interactions occurred. Palmitic acid formed eight hydrogen bonds with four residues, namely Gln-59, Lys-24, Phe-55, and Tyr-56. Palmitic acid also formed two Pi-Alkyl interactions with Phe-55 and Tyr-56 residues. The finding demonstrated that caspase-3 bound to palmitic acid and linolenyl alcohol, with binding energies of -3.56 kcal/mol and -3.93 kcal/mol, respectively. Mutazah et al. [57] previously reported that entadamide C (1) and clinamide D (2) from *C. nutans* extracts bound favorably to the caspase-3 binding site, with binding energies of -4.28 kcal/mol and -4.84 kcal/mol, respectively. Thus, these results showed that such interactions of *C. nutans* compounds are important for the activation of apoptosis-related proteins.

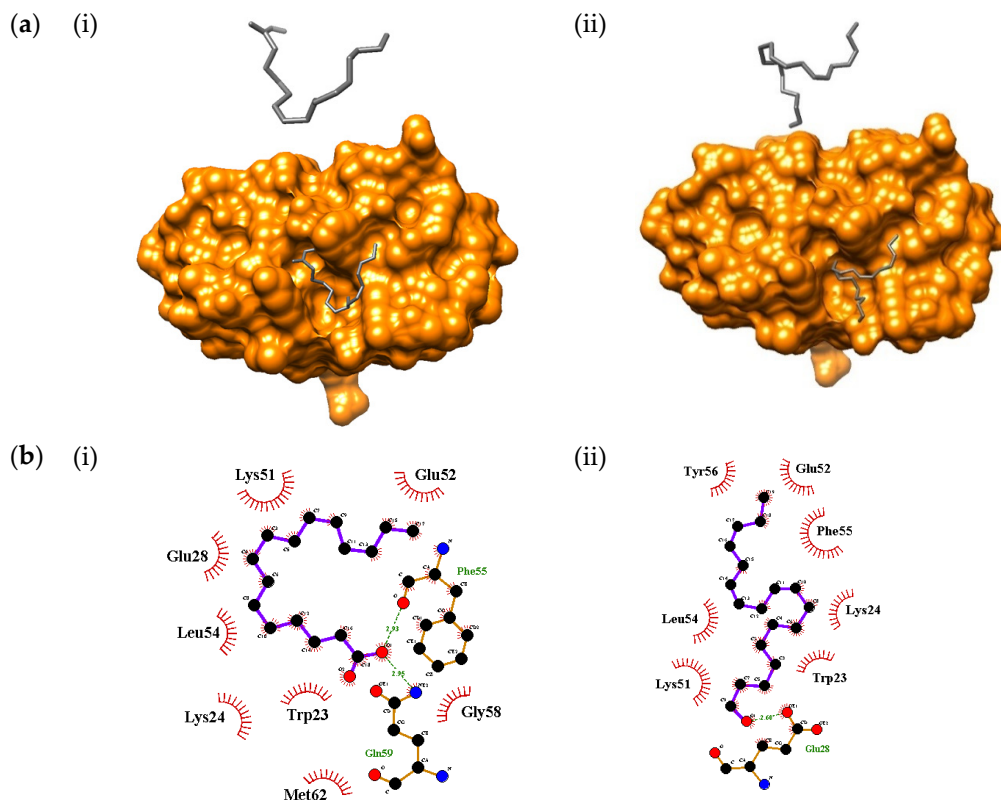


Figure 4. Cont.

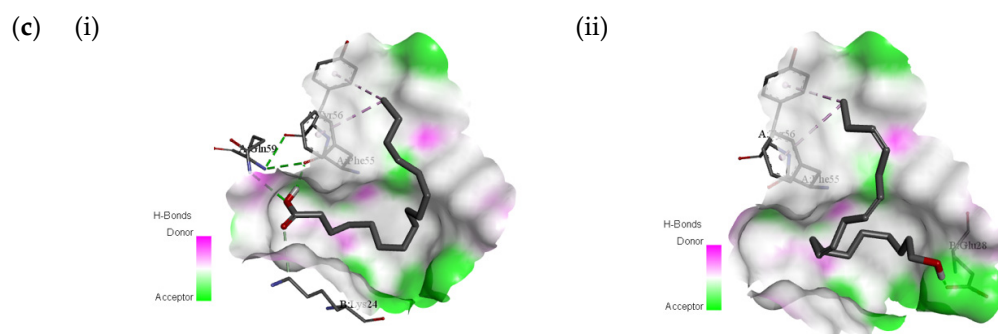


Figure 4. Molecular docking and interaction pattern analysis of the compounds with apoptosis proteins: (a) the best binding affinities of the compounds with targeted proteins; (b) interaction of the compounds and active site residues using LigPlot+; (c) interaction of the compounds with active site residues using Discovery Studio Visualizer 4.1 client. The compounds and proteins correspond to (i) palmitic acid with p53-binding protein Mdm-2 and (ii) linolenyl alcohol with p53-binding protein Mdm-2.

3. Materials and Methods

3.1. Reagents

Analytical grade methanol, hexane, dichloromethane, chloroform, *n*-butanol, dimethylsulfoxide (DMSO), acetic acid, and HPLC-grade methanol were purchased from Qrec (Asia) Sdn. Bhd (Rawang, Selangor, Malaysia). Folin–Ciocalteu reagent, sodium carbonate, DPPH, ABTS, aluminum chloride, potassium persulfate, sulforhodamine B, tris buffer, and trichloroacetic acid were purchased from Sigma-Aldrich (St. Louis, MO, USA). The standards for antioxidant assays (quercetin, gallic acid, and vitamin E analogue 6-hydroxy 2,5,7,8-tetramethylchroman-2-carboxylic acid (Trolox)) were purchased from Sigma-Aldrich (St. Louis, MO, USA). Roswell Park Memorial Institute culture medium (RPMI-1640) and fetal bovine serum were purchased from Nacalai Tesque (Kyoto, Japan). Dulbecco’s modified Eagle medium (DMEM), penicillin-streptomycin (PenStrep), horse serum, epidermal growth factor (EGF), hydrocortisone, and insulin were purchased from Gibco (Paisley, UK). Trypan blue was purchased from Hyclon de México (Zapopan, México).

3.2. Plant Material and Sample Preparation

Fresh samples of *C. nutans* were purchased from HERBagus at Kepala Batas, Penang, Malaysia (5.5185° N, 100.4799° E), and the plant was identified using DNA barcoding markers [9]. The leaves were separated from the plants and washed with distilled water. Fresh leaves (3000 g) were ground and soaked with 80% methanol (2.5 L) at room temperature (20 °C). The mixtures were continuously shaken at 130 rpm for 24 h on a shaker. The filtrate was collected by filtration of the mixtures through a Whatman No. 1 filter paper by gravity. The extraction was repeated two more times and the crude extracts were pooled together. Methanol was evaporated from the pooled crude extract using a rotary evaporator (125 hpa, 40 °C) and the crude extract was freeze-dried.

Next, 70 g of crude extract were dissolved with distilled water (100 mL) and subjected to liquid–liquid fractionation with each of the following four solvents (200 mL) of different polarities: *n*-hexane (CN-Hex), dichloromethane (Cn-Dcm), chloroform (CN-Chl), and *n*-butanol (CN-But) (Figure 5). The mixtures were mixed vigorously with the solvents (200 mL) in a separatory funnel for 30 min. The extraction solvents were evaporated from the fractions, and water was also evaporated. All samples were kept at 4 °C until further use.

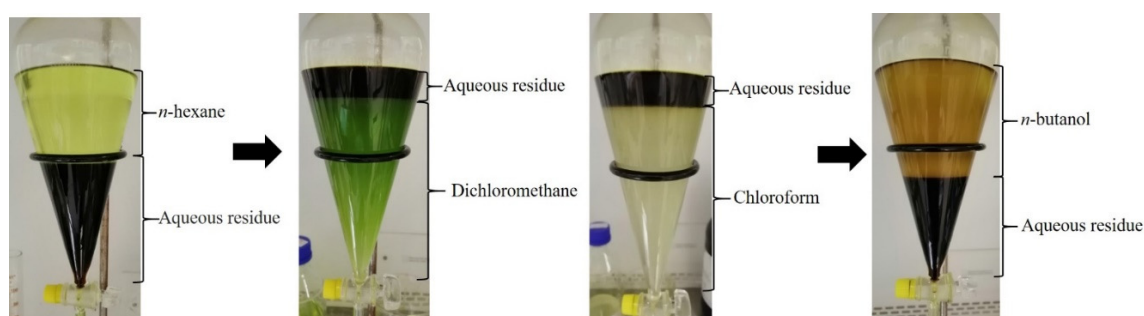


Figure 5. Fractionation of crude extracts using four solvents of different polarities (*n*-hexane, dichloromethane, chloroform, and *n*-butanol, along with aqueous residue).

3.3. Determination of Antioxidant Activities

3.3.1. TPC

The TPC of *C. nutans* crude and fraction extracts was measured following Ismail et al. [28], with slight modification. First, 1000 μg of each extract were diluted using 50% methanol to obtain 1000 $\mu\text{g}/\text{mL}$ of sample concentration and then 1 mL of 100% Folin–Ciocalteu reagent was mixed with 9 mL of distilled water. Next, 0.3 g of sodium carbonate was dissolved in 4 mL of distilled water to obtain 7.5% sodium carbonate. The extracts (20 μL) were added to 96-well plates and mixed with 100 μL of 10% Folin–Ciocalteu reagent. The mixtures were incubated for 5 min in the dark. Next, 80 μL of 7.5% sodium carbonate were added to the mixtures, which were incubated for 30 min before reading the absorbance at 760 nm using a spectrophotometer (OMEGA BMG Labtech, Ortenberg, Germany). The analysis was performed in triplicate. A total of nine concentrations of gallic acid ranging from 3.9 to 1000 $\mu\text{g}/\text{mL}$ were made by serial dilution. The same procedure was repeated for the gallic acid concentrations and the calibration line was created. The TPC was expressed as percentage of total gallic acid equivalents per g extract (mg GAE/g). The TPC regression curve for the gallic acid standard had the equation $y = 0.0076x - 0.0031$, with an R^2 value of 0.9999.

3.3.2. TFC

The TFC of *C. nutans* crude and fraction extracts was measured following Ismail et al. [28]. A 100 μL aliquot of the prepared solutions (1000 $\mu\text{g}/\text{mL}$) of crude and fraction extracts of *C. nutans* leaves was added to 100 μL of 2% aluminum chloride and incubated for 10 min in the dark. The absorbance of the mixture then was read using a spectrophotometer at 420 nm. The analysis was performed in triplicate. Serial dilutions of the standard quercetin starting from 1000 $\mu\text{g}/\text{mL}$ were used to generate a standard curve. The TFC was expressed as percentage of total quercetin equivalents per g extract (mg QE/g). The TFC regression curve for the quercetin standard had the equation $y = 0.0107x + 0.0272$, with an R^2 value of 0.9989.

3.3.3. DPPH

The antioxidant capacity was measured using the DPPH radical scavenging method, as described by Ismail et al. [28], with some modifications. A 0.6 mM DPPH stock solution was prepared by dissolving 6 mg of DPPH in 25 mL of methanol. The DPPH working solution was obtained by dissolving the DPPH stock solution in methanol until the absorbance reading at 517 nm was 1.1 ± 0.02 nm. Next, 50 μL of the *C. nutans* crude and fraction extracts ranging from concentrations of 125 to 4000 $\mu\text{g}/\text{mL}$ were added to 100 μL of DPPH working solution in 96-well plates. The mixtures were incubated at 30 min in the dark. The absorbance was read at 517 nm using the spectrophotometer. Trolox ranging from 3.9 to 1000 $\mu\text{g}/\text{mL}$ was used as a positive control. The experiment was performed in triplicate for the standard and the extracts. The inhibition ratio was calculated as percentage of inhibition using the following formula: percentage inhibition (%) = ((absorbance of control) – (absorbance of test

sample)/absorbance of control) \times 100%. The extract concentration providing the half-maximal effective concentration (EC₅₀) was calculated using a graph by plotting the percentage effective concentration against extract concentration. The data were presented as mean values \pm standard deviation (SD).

3.3.4. ABTS

The ABTS radical cation decolorization assay described by Fidrianny et al. [58] was used. The ABTS radical cation working solution was produced by reacting 7.5 mM ABTS stock solution with 3.8 mM potassium persulfate, and the mixture was allowed to stand in the dark at room temperature for 16 h before use to yield a dark-colored solution containing ABTS \bullet + radicals. The ABTS radical cation working solution was then diluted with methanol for an initial absorbance of about 0.70 ± 0.02 at 734 nm. Mixtures in a total volume of 100 μ L containing 90 μ L of ABTS radical cation working solution and 10 μ L of varying concentrations of the extract (125–4000 μ g/mL) were incubated in the dark. Appropriate solvent blanks were run with each assay. The absorbance was read by the spectrophotometer at 734 nm and compared with the Trolox control (3.9–1000 μ g/mL). The assay was performed in triplicate. The scavenging activity was estimated based on the EC₅₀ of ABTS radicals scavenged. The data were presented as mean values \pm SD.

3.3.5. Statistical Analysis

All the experiments for determination of TPC, TFC, and antioxidant properties using DPPH and ABTS were conducted in triplicates. The values are expressed as the mean \pm standard deviation (SD). The statistical analysis of the results was done by IBM Statistical Package for Social Sciences (SPSS) Statistical Version 24 for statistical computing. Analysis of variance (ANOVA) and significance of differences among means were tested by one-way ANOVA and least significant difference (LSD) on mean values, respectively.

3.4. Cell Culture for Cytotoxicity Testing

Cryovials containing MCF7 and MCF 10A cells were thawed in a water bath at 37 °C. The cells were then transferred into a 15 mL centrifuge tube and centrifuged at 1000 rpm for 5 min to remove the cryopreservative agent (DMSO). The MCF7 cells were introduced into a T-25 falcon flask and cultivated in RPMI-1640 medium supplemented with 10% (*v/v*) fetal bovine serum and 1% PenStrep to increase and stimulate cells survival and proliferation. PenStrep was added to preferentially kill any bacteria present that might contaminate the cells. The MCF 10A were cultivated in DMEM supplemented with 5% horse serum, 20 mg/mL epidermal growth factor, 0.5 mg/mL hydrocortisone, 10 μ g/mL insulin, and 5 mL of PenStrep. Both cell types were incubated at 37 °C in a CO₂ incubator supplemented with 5% CO₂. The media were replaced every 3 days until the cells were confluent and ready to be sub-cultivated. The medium in each flask was discarded when the cells reached confluence. The cells were then washed two times with 2 mL of phosphate-buffered saline to ensure removal of any residue of spent culture medium and dead cells. Cells were detached by adding 200 μ L of trypsin and incubated for 5 min. The process of trypsinization was enhanced by gently tapping the flask a few times. Once the cells appeared rounded and single under the microscope, 4 mL of medium were added to the cells to inactivate the trypsin. The cell suspension was transferred to a 15 mL falcon tube and centrifuged at 1000 rpm for 5 min. Cells then were resuspended in the culture media.

3.4.1. Cell Viability Assay

The effects of *C. nutans* crude extract and its fractions on the viability of MCF7 and MCF 10A cells were determined using the sulforhodamine B (SRB) assay, as described by Skehan et al. [34], with some modifications. Concentrations of MCF7 and MCF 10A cells growing in the exponential phase (1×10^4 cells/mL) were produced using an automated cell counter. Aliquots of 100 μ L of medium were seeded into each well of 96-well plates and incubated in a CO₂ incubator for 24 h. The CN-Crd extract and CN-Aqu residue extract were dissolved in both complete media, whereas CN-Hex, CN-Dcm,

CN-Chl, and CN-But fractions were dissolved in DMSO. The working solutions of fraction extracts were in 0.1% DMSO. This was to make sure that the highest DMSO concentration in the cell culture was within the acceptable limit (0.1–0.5%) [59]. Briefly, the cells were incubated in 96-well plates with a serial dilution of extracts, starting with 1000 µg/mL (CN-Crd and CN-Aqu) and 300 µg/mL (CN-Hex, CN-Dcm, CN-Chl, and CN-But fraction extracts) for 72 h at 37 °C with 5% CO₂.

For MCF 10A cells, the new range of crude and fraction extracts of *C. nutans* leaves was made based on the half-maximal inhibitory concentration (IC₅₀) of MCF7 cancer cells. The new range for MCF 10A cells started with 500 µg/mL (CN-Crd and CN-Aqu) and 120 µg/mL (CN-Hex, CN-Dcm, CN-Chl, and CN-But fraction extracts). The positive control experiment involved tamoxifen, and the negative control was untreated media or 0.1% DMSO. At the end of the incubation period, the cells were fixed with 50 µL of 50% cold trichloroacetic acid for 30 min at room temperature, followed by gentle tap water washing (4x) and drying. The cells then were then stained with 100 µL of 0.4% SRB in 1% acetic acid for 30 min, followed by washing with 1% acetic acid (4x). The plate was dried, 100 µL of 10 mM Tris buffer were added to each well, and the plate was shaken for 5 min. Relative cell viability was measured by scanning at 570 nm on a microplate reader (OMEGA BMG Labtech, Subang Jaya, Selangor, Malaysia). The cytotoxicity was determined using the previously described formula reported by Bendale et al. [60]:

$$\text{Cytotoxicity (\%)} = \text{Optical density of (sample - blank)} / \text{Optical density of (control - blank)} \times 100\% \quad (1)$$

3.4.2. Selective Index (SI)

The SI was used to determine the cytotoxic selectivity of the substances tested. It was calculated according to the following equation [61]:

$$\text{SI} = \text{IC}_{50} (\text{normal cells}) / \text{IC}_{50} (\text{cancer cells}) \quad (2)$$

The extract with highest SI (CN-Dcm) was selected for another cell viability assay at different incubation times (24, 48, and 72 h).

3.5. GC-MS

For the GC-MS analysis, 1000 µg/mL of CN-Dcm was dissolved in 1 mL of HPLC grade methanol. The secondary metabolites from CN-Dcm were determined using an Agilent gas chromatograph model 6890 equipped with an Agilent 19091S-433 capillary column, (5%-phenyl)-methylpolysiloxane phase (HP-5MS) 0.25 mm × 30 m × 0.25 µm (Santa Clara, CA, USA). Helium gas was used as the carrier gas at 1.0 mL per minute with split mode injection. The oven temperature was set as follows: 70 °C was held for 2 min, then it was increased to 280 °C at a rate of 20 °C per min for 20 min. The total run time was 32.50 min.

3.6. Molecular Docking

3.6.1. Drug-Likeness and Toxicity Predictions

Lipinski's rule of five was used to predict the drug-likeness; this rule determines the consistency of orally active drugs [45,47]. In this study, the selected compounds (palmitic acid linolenyl alcohol) were screened using the SwissADME web tool predictor [62]. The SwissADME predictor provides data on the numbers of hydrogen acceptors, hydrogen donors, and rotatable bonds.

3.6.2. Protein Model and Compound Structure

Protein structures of tumor necrosis factor alpha (TNF-α, PDB ID: 2AZ5), p53-binding protein Mdm-2 (PDB ID: 1YCR), and caspase-3 (PDB ID: 6CKZ) were retrieved from the Research Collaboratory Structural Bioinformatics Protein Data Bank. All data files were saved in .pdb file format. Water and

ligand molecules from the proteins were removed using Discovery Studio Visualizer 4.1 client [63]. The selected compounds (palmitic acid linolenyl alcohol) were structured using Advanced Chemistry Development/ChemSketch (ACD/ChemSketch) freeware [64]. The generated structures were saved in .mol2 file format, which then was converted to .pdb file format using Open Babel: The Open Source Chemistry Toolbox.

3.6.3. Molecular Docking Analysis

Molecular docking analysis was conducted using the automated docking tool AutoDock 4.2 [65]. Polar hydrogen atoms and Gasteiger partial charges were added to the three-dimensional protein structure. The protein structure was written in .pdbqt file format for further analysis. In this study, the grid size was set at $40 \times 40 \times 40$ points, with 0.375 \AA spacing centered on TNF- α , with grid centers $x (-13.687)$, $y (71.607)$, and $z (27.002)$; $40 \times 40 \times 40$ points with 0.375 \AA spacing centered on p53-binding protein Mdm-2, with grid centers $x (22.407)$, $y (-17.053)$, and $z (-7.329)$; and $40 \times 40 \times 40$ points with 0.375 \AA spacing centered on caspase-3, with grid centers $x (27.543)$, $y (22.594)$, and $z (37.217)$. Lamarckian Genetic Algorithm 4.2 was used in the docking analysis [66] and the protein macromolecules were kept rigid throughout the docking simulation. Genetic algorithm runs were set at 100 and the other parameters for docking analyses were left at default settings. The best protein–compound conformations were chosen from the AutoDock 4.2 scoring function, and they were ranked according to their binding affinities. Discovery Studio Visualizer 4.1 client [63], Chimera 1.14 [67], and LigPlot [68] were used for post-docking analyses.

4. Conclusions

The TPC, TFC, antioxidant scavenging activity, antiproliferative activities, and molecular docking of *C. nutans* leaf extracts were determined in this study. The TPC of *C. nutans* leaf extracts was higher than that of TFC. In addition, the CN-Hex fraction had the lowest antioxidant activity and the CN-Crd fraction had the highest antioxidant activity based on the EC_{50} value. The CN-Dcm extract was chosen to study the antiproliferative effect of the leaf extract because it inhibited MCF7 cell growth and was less toxic towards MCF 10A cells. Molecular docking results showed that palmitic acid and linolenyl alcohol from the CN-Dcm fraction could bind with three selected apoptosis-related proteins, and that p53-binding protein Mdm-2 had the highest binding affinity with both compounds. These results suggest that CN-Dcm would be useful for identifying the compounds that best inhibit proliferation of cancer cells and in other applications for determining the apoptosis signaling pathway. For future studies, we would like to isolate and purify the potential active compounds from CN-Dcm fractions. Moreover, it would be worthwhile if we investigated the active compound activity against apoptosis analysis using RNA and protein expression.

Supplementary Materials: The following are available online: Table S1: The IC_{50} of *C. nutans* extracts using sulforhodamine B (SRB), 3-(4,5-dimethylthiazol-2-yl)-5-(3-carboxymethoxyphenyl)-2-(4-sulfophenyl)-2H-tetrazolium (MTS), and alamar blue assays at 72 h exposure. The antiproliferative effects were evaluated by using MCF7 and MCF 10A.

Author Contributions: Conceptualization, N.Z.I. and H.A.; data curation, N.Z.I. and H.A.; formal analysis, N.Z.I. and Z.M.T.; funding acquisition, H.A.; investigation, N.Z.I.; methodology, N.Z.I., Z.M.T., and M.M.; project administration, M.M. and H.A.; resources, N.N.S.N.M.K. and N.N.M.Z.; software, N.Z.I.; supervision, N.N.M.Z. and H.A.; validation, N.Z.I., Z.M.T., M.M., and H.A.; visualization, N.Z.I.; writing—original draft, N.Z.I.; writing—review and editing, N.Z.I. and H.A. All authors have read and agreed to the published version of the manuscript.

Funding: This research was funded by Universiti Sains Malaysia Bridging Grant, grant number 304/CIPPT/6316239.

Acknowledgments: The first author gratefully acknowledges Universiti Sains Malaysia (USM) for fellowship under the USM Fellowship Scheme.

Conflicts of Interest: The authors declare no conflict of interest.

References

1. El-Saied, F.; El-Aarag, B.; Salem, T.; Said, G.; Khalifa, S.A.; El-Seedi, H.R. Synthesis, characterization, and in vivo anti-cancer activity of new metal complexes derived from isatin-N (4) antipyrinethiosemicarbazone ligand against ehrlich ascites carcinoma cells. *Molecules* **2019**, *24*, 3313. [[CrossRef](#)] [[PubMed](#)]
2. Reed, J.C. Dysregulation of apoptosis in cancer. *J. Clin. Oncol.* **1999**, *17*, 2941. [[CrossRef](#)] [[PubMed](#)]
3. Ferlay, J.; Soerjomataram, I.; Dikshit, R.; Eser, S.; Mathers, C.; Rebelo, M.; Parkin, D.M.; Forman, D.; Bray, F. Cancer incidence and mortality worldwide: Sources, methods and major patterns in GLOBOCAN 2012. *Int. J. Cancer* **2015**, *136*, 359–386. [[CrossRef](#)] [[PubMed](#)]
4. Hisham, A.N.; Yip, C.H. Overview of breast cancer in Malaysian women: A problem with late diagnosis. *Asian J. Surg.* **2004**, *27*, 130–133. [[CrossRef](#)]
5. Sak, K. Chemotherapy and dietary phytochemical agents. *Chemother. Res. Pract.* **2012**, *2012*, 1–11. [[CrossRef](#)]
6. Siddiqui, M.; Rajkumar, S.V. The high cost of cancer drugs and what we can do about it. *Mayo Clin. Proc.* **2012**, *87*, 935–943. [[CrossRef](#)]
7. Yeo, B.S.; Yap, Y.J.; Koh, R.Y.; Ng, K.Y.; Chye, S.M. Medicinal properties of *Clinacanthus nutans*: A review. *Trop. J. Pharm. Res.* **2018**, *17*, 375–382. [[CrossRef](#)]
8. Chelyn, J.L.; Omar, M.H.; Yousof, M.; Akmal, N.S.; Ranggassamy, R.; Wasiman, M.I.; Ismail, Z. Analysis of flavone C-glycosides in the leaves of *Clinacanthus nutans* (Burm. f.) Lindau by HPTLC and HPLC-UV/DAD. *Sci. World J.* **2014**, *2014*, 1–7. [[CrossRef](#)]
9. Ismail, N.Z.; Arsad, H.; Samian, M.R.; Hamdan, M.R.; Othman, A.S. Assessment of three plastid DNA barcode markers for identification of *Clinacanthus nutans* (Acanthaceae). *3 Biotech* **2018**, *8*, 1–8. [[CrossRef](#)]
10. Alam, A.; Ferdosh, S.; Ghafoor, K.; Hakim, A.; Juraimi, A.S.; Khatib, A.; Sarker, Z.I. *Clinacanthus nutans*: A review of the medicinal uses, pharmacology and phytochemistry. *Asian Pac. J. Trop. Biomed.* **2016**, *9*, 402–409. [[CrossRef](#)]
11. Levenson, A.S.; Jordan, V.C. MCF-7: The first hormone-responsive breast cancer cell line. *Cancer Res.* **1997**, *57*, 3071–3078.
12. Holliday, D.L.; Speirs, V. Choosing the right cell line for breast cancer research. *Breast Cancer Res.* **2011**, *13*, 1–7. [[CrossRef](#)] [[PubMed](#)]
13. Christgen, M.; Lehmann, U. MDA-MB-435: The questionable use of a melanoma cell line as a model for human breast cancer is ongoing. *Cancer Biol. Ther.* **2007**, *6*, 1351–1353. [[CrossRef](#)] [[PubMed](#)]
14. Robertson, J.F.; Osborne, C.K.; Howell, A.; Jones, S.E.; Mauriac, L.; Ellis, M.; Kleeberg, U.R.; Come, S.E.; Vergote, I.; Gertler, S.; et al. Fulvestrant versus anastrozole for the treatment of advanced breast carcinoma in postmenopausal women: A prospective combined analysis of two multicenter trials. *Cancer* **2003**, *98*, 229–238. [[CrossRef](#)] [[PubMed](#)]
15. Majeed, M.; Hussain, A.I.; Chatha, S.A.; Khosa, M.K.; Kamal, G.M.; Kamal, M.A.; Zhang, X.; Liu, M. Optimization protocol for the extraction of antioxidant components from *Origanum vulgare* leaves using response surface methodology. *Saudi J. Biol. Sci.* **2016**, *23*, 389–396. [[CrossRef](#)]
16. Dai, J.; Mumper, R.J. Plant phenolics: Extraction, analysis and their antioxidant and anticancer properties. *Molecules* **2010**, *15*, 7313–7352. [[CrossRef](#)]
17. Haron, N.H.; Abas, R.; Md Toha, Z.; Hamdam, M.R.; Azman, N.; Samian, M.R.; Arsad, H. Effect of different solvent extracts on phenolic, flavonoid and antioxidant content and antiproliferative activity of *Clinacanthus nutans* leaves extract. In Proceedings of the 41st Annual Conference of the Malaysian Society for Biochemistry and Molecular Biology, Pullman Kuala Lumpur Bangsar Hotel, Bangsar, Kuala Lumpur, Malaysia, 18 August 2016.
18. Sarega, N.; Imam, M.U.; Ooi, D.J.; Chan, K.W.; Md Esa, N.; Zawawi, N.; Ismail, M. Phenolic rich extract from *Clinacanthus nutans* attenuates hyperlipidemia-associated oxidative stress in rats. *Oxidative Med. Cell. Longev.* **2016**, 1–16. [[CrossRef](#)]
19. Aliyu, A.; Ibrahim, M.; Musa, A.; Bulus, T.; Oyewale, A. Phenolics content and antioxidant capacity of extracts and fractions of *Vernonia blumeoides* (Asteraceae). *Int. J. Biol. Chem.* **2011**, *5*, 352–359. [[CrossRef](#)]
20. Johari, M.A.; Khong, H.Y. Total phenolic content and antioxidant and antibacterial activities of *Pereskia bleo*. *Adv. Pharm. Sci.* **2019**, *2019*, 1–4. [[CrossRef](#)]

21. Sakanaka, S.; Ishihara, Y. Comparison of antioxidant properties of persimmon vinegar and some other commercial vinegars in radical-scavenging assays and on lipid oxidation in tuna homogenates. *Food Chem.* **2008**, *107*, 739–744. [[CrossRef](#)]
22. Kumar, A.; Premoli, M.; Aria, F.; Bonini, S.A.; Maccarinelli, G.; Gianoncelli, A.; Memo, M.; Mastinu, A. Cannabimimetic plants: Are they new cannabinoidergic modulators? *Planta* **2019**, *249*, 1681–1694. [[CrossRef](#)] [[PubMed](#)]
23. Premoli, M.; Aria, F.; Bonini, S.A.; Maccarinelli, G.; Gianoncelli, A.; Della Pina, S.; Tambaro, S.; Memo, M.; Mastinu, A. Cannabidiol: Recent advances and new insights for neuropsychiatric disorders treatment. *Life Sci.* **2019**, *224*, 120–127. [[CrossRef](#)] [[PubMed](#)]
24. Suriyatem, R.; Auras, R.A.; Intipunya, P.; Rachtanapun, P. Predictive mathematical modeling for EC50 calculation of antioxidant activity and antibacterial ability of Thai bee products. *J. Appl. Pharm. Sci.* **2017**, *7*, 122–133. [[CrossRef](#)]
25. Lachman, J.; Orsák, M.; Hejtmánková, A.; Kovářová, E. Evaluation of antioxidant activity and total phenolics of selected Czech honeys. *Lwt Food Sci. Technol.* **2010**, *43*, 52–58. [[CrossRef](#)]
26. Olugbami, J.O.; Gbadegehin, M.A.; Odunola, O.A. In vitro free radical scavenging and antioxidant properties of ethanol extract of *Terminalia glaucescens*. *Phcog. Res.* **2015**, *7*, 49–56. [[CrossRef](#)]
27. Alam, M.A.; Zaidul, I.; Ghafoor, K.; Sahena, F.; Hakim, M.; Rafii, M.; Abir, H.; Bostanudin, M.; Perumal, V.; Khatib, A. In vitro antioxidant and, α -glucosidase inhibitory activities and comprehensive metabolite profiling of methanol extract and its fractions from *Clinacanthus nutans*. *Bmc Complement. Altern. Med.* **2017**, *17*, 1–10. [[CrossRef](#)]
28. Ismail, N.Z.; Arsad, H.; Samian, M.R.; Hamdan, M.R. Determination of phenolic and flavonoid contents, antioxidant activities and GC-MS analysis of *Clinacanthus nutans* (Acanthaceae) in different locations. *Agrivita J. Agric. Sci.* **2017**, *39*, 335–344. [[CrossRef](#)]
29. Ismail, N.Z.; Arsad, H.; Samian, M.R.; Ab Majid, A.H.; Hamdan, M.R. Evaluation of genetic diversity of *Clinacanthus nutans* (Acanthaceae) using RAPD, ISSR and RAMP markers. *Physiol. Mol. Biol. Plants* **2016**, *22*, 523–534. [[CrossRef](#)]
30. Kuete, V.; Karaosmanoğlu, O.; Sivas, H. Anticancer activities of African medicinal spices and vegetables. In *Medicinal Spices and Vegetables from Africa*; Academic Press: London, UK, 2017; pp. 271–297.
31. Aslantürk, Ö.S. Genotoxicity—A predictable risk to our actual world. In *In Vitro Cytotoxicity and Cell Viability Assays: Principles, Advantages, and Disadvantages*, 1st ed.; Larramendy, M., Soloneski, S., Eds.; IntechOpen: London, UK, 2018; Volume 3, pp. 1–19. [[CrossRef](#)]
32. Vajrabhaya, L.O.; Korsuwannawong, S. Cytotoxicity evaluation of *Clinacanthus nutans* through dimethylthiazol diphenyltetrazolium bromide and neutral red uptake assays. *Eur. J. Dent.* **2016**, *10*, 134–138. [[CrossRef](#)]
33. Van Tonder, A.; Joubert, A.M.; Cromarty, A.D. Limitations of the 3-(4, 5-dimethylthiazol-2-yl)-2, 5-diphenyl-2H-tetrazolium bromide (MTT) assay when compared to three commonly used cell enumeration assays. *BMC Res. Notes* **2015**, *8*, 1–10. [[CrossRef](#)]
34. Skehan, P.; Storeng, R.; Scudiero, D.; Monks, A.; McMahon, J.; Vistica, D.; Warren, J.T.; Bokesch, H.; Kenney, S.; Boyd, M.R. New colorimetric cytotoxicity assay for anticancer-drug screening. *J. Natl. Cancer Inst.* **1990**, *82*, 1107–1112. [[CrossRef](#)] [[PubMed](#)]
35. Arullappan, S.; Rajamanickam, P.; Thevar, N.; Kodimani, C.C. In vitro screening of cytotoxic, antimicrobial and antioxidant activities of *Clinacanthus nutans* (Acanthaceae) leaf extracts. *Trop. J. Pharm. Res.* **2014**, *13*, 1455–1461. [[CrossRef](#)]
36. Haron, N.H.; Md Toha, Z.; Abas, R.; Hamdan, M.R.; Azman, N.; Khairuddean, M.; Arsad, H. In vitro cytotoxic activity of *Clinacanthus nutans* leaf extracts against HeLa cells. *Asian Pac. J. Cancer* **2019**, *20*, 601–609. [[CrossRef](#)] [[PubMed](#)]
37. Adebayo, I.A.; Arsad, H.; Samian, M.R. Antiproliferative effect on breast cancer (MCF7) of *Moringa oleifera* seed extracts. *Afr. J. Tradit. Complement. Altern. Med.* **2017**, *14*, 282–287. [[CrossRef](#)] [[PubMed](#)]
38. Tagne, R.S.; Telefo, B.P.; Talla, E.; Nyemb, J.N.; Njina, S.N.; Asrar, M.; Mukhtar, F.; Kamdje, A.H.N.; Moundipa, P.F.; Farooq, A.D. Bio-guided fractionation of methanol extract of *Ziziphus mauritiana* Lam.(bark) and effect of the most active fraction on cancer cell lines. *Asian Pac. J. Trop. Dis.* **2015**, *5*, 307–312. [[CrossRef](#)]

39. Wang, K.S.; Chan, C.K.; Hidayat, A.F.A.; Wong, Y.H.; Kadir, H.A. *Clinacanthus nutans* induced reactive oxygen species-dependent apoptosis and autophagy in HCT116 human colorectal cancer cells. *Pharm. Mag.* **2019**, *15*, 87–97. [[CrossRef](#)]
40. Segun, P.A.; Ogbale, O.O.; Ismail, F.M.; Nahar, L.; Evans, A.R.; Ajaiyeoba, E.O.; Sarker, S.D. Resveratrol derivatives from *Commiphora africana* (A. Rich.) Endl. display cytotoxicity and selectivity against several human cancer cell lines. *Phytother. Res.* **2019**, *33*, 159–166. [[CrossRef](#)]
41. Ng, P.Y.; Chye, S.M.; Ng, C.H.; Koh, R.Y.; Tiong, Y.L.; Pui, L.P.; Tan, Y.H.; Lim, C.S.Y.; Ng, K.Y. *Clinacanthus nutans* hexane extracts induce apoptosis through a caspase-dependent pathway in human cancer cell lines. *Asian Pac. J. Cancer Prev.* **2017**, *18*, 917–926. [[CrossRef](#)]
42. Sulaiman, I.S.C.; Basri, M.; Chan, K.W.; Ashari, S.E.; Masoumi, H.R.F.; Ismail, M. In vitro antioxidant, cytotoxic and phytochemical studies of *Clinacanthus nutans* Lindau leaf extracts. *Afr. J. Pharm. Pharm.* **2015**, *9*, 861–874. [[CrossRef](#)]
43. Yong, Y.K.; Tan, J.J.; Teh, S.S.; Mah, S.H.; Ee, G.C.L.; Chiong, H.S.; Ahmad, Z. *Clinacanthus nutans* extracts are antioxidant with antiproliferative effect on cultured human cancer cell lines. *Evid. Based Complement. Altern. Med.* **2013**, *2013*, 1–8. [[CrossRef](#)]
44. Fadeyi, S.A.; Fadeyi, O.O.; Adejumo, A.A.; Okoro, C.; Myles, E.L. In vitro anticancer screening of 24 locally used Nigerian medicinal plants. *Bmc Complement. Altern. Med.* **2013**, *13*, 1–10. [[CrossRef](#)] [[PubMed](#)]
45. Lipinski, C.A. Lead and drug-like compounds: The rule-of-five revolution. *Drug Discov. Today Technol.* **2004**, *1*, 337–341. [[CrossRef](#)] [[PubMed](#)]
46. Oduselu, G.O.; Ajani, O.O.; Ajamma, Y.U.; Brors, B.; Adebisi, E. Homology modelling and molecular docking studies of selected substituted Benzo [d] imidazol-1-yl) methyl) benzimidamide scaffolds on *Plasmodium falciparum* adenylosuccinate lyase receptor. *Bioinform. Biol. Insights* **2019**, *13*, 1–10. [[CrossRef](#)] [[PubMed](#)]
47. Lipinski, C.A.; Lombardo, F.; Dominy, B.W.; Feeney, P.J. Experimental and computational approaches to estimate solubility and permeability in drug discovery and development settings. *Adv. Drug Deliv. Rev.* **1997**, *23*, 3–25. [[CrossRef](#)]
48. Sethi, A.; Joshi, K.; Sasikala, K.; Alvala, M. Molecular docking in modern drug discovery: Principles and recent applications. In *Drug Discovery and Development-New Advances*; IntechOpen: London, UK, 2019; pp. 1–22.
49. Elmore, S. Apoptosis: A review of programmed cell death. *Toxicol. Pathol.* **2007**, *35*, 495–516. [[CrossRef](#)]
50. Adebayo, I.A.; Balogun, W.G.; Arsal, H. *Moringa oleifera*: An apoptosis inducer in cancer cells. *Trop. J. Pharm. Res.* **2017**, *16*, 2289–2296. [[CrossRef](#)]
51. Amaral, J.D.; Xavier, J.M.; Steer, C.J.; Rodrigues, C.M. The role of p53 in apoptosis. *Discov. Med.* **2010**, *9*, 145–152.
52. Adebayo, I.A.; Arsal, H.; Samian, M.R. Methyl elaidate: A major compound of potential anticancer extract of *Moringa oleifera* seeds binds with bax and MDM2 (p53 inhibitor) in silico. *Pharm. Mag.* **2018**, *14*, 554–557. [[CrossRef](#)]
53. Leão, M.; Pereira, C.; Bisio, A.; Ciribilli, Y.; Paiva, A.M.; Machado, N.; Palmeira, A.; Fernandes, M.X.; Sousa, E.; Pinto, M. Discovery of a new small-molecule inhibitor of p53–MDM2 interaction using a yeast-based approach. *Biochem. Pharm.* **2013**, *85*, 1234–1245. [[CrossRef](#)]
54. Álvarez, S.; Blanco, A.; Fresno, M.; Muñoz-Fernández, M.Á. TNF- α contributes to caspase-3 independent apoptosis in neuroblastoma cells: Role of NFAT. *PLoS ONE* **2011**, *6*, 1–13. [[CrossRef](#)]
55. Porter, A.G.; Jänicke, R.U. Emerging roles of caspase-3 in apoptosis. *Cell Death Differ.* **1999**, *6*, 99–104. [[CrossRef](#)] [[PubMed](#)]
56. Pansar, T.; Poso, A. Binding affinity via docking: Fact and fiction. *Molecules* **2018**, *23*, 1899. [[CrossRef](#)] [[PubMed](#)]
57. Mutazah, R.; Hamid, H.A.; Ramli, A.N.M.; Aluwi, M.F.F.M.; Yusoff, M.M. In vitro cytotoxicity of *Clinacanthus nutans* fractions on breast cancer cells and molecular docking study of sulphur containing compounds against caspase-3. *Food Chem. Toxicol.* **2019**, *135*, 1–9. [[CrossRef](#)] [[PubMed](#)]
58. Fidrianny, I.; Rahmiyani, I.; Wirasutisna, K.R. Antioxidant capacities from various leaves extracts of four varieties mangoes using DPPH, ABTS assays and correlation with total phenolic, flavonoid, carotenoid. *Int. J. Pharm. Pharm. Sci.* **2013**, *5*, 189–194. [[CrossRef](#)]

59. Scambia, G.; Ranelletti, F.; Panici, P.B.; De Vincenzo, R.; Bonanno, G.; Ferrandina, G.; Piantelli, M.; Bussa, S.; Rumi, C.; Cianfriglia, M. Quercetin potentiates the effect of adriamycin in a multidrug-resistant MCF-7 human breast-cancer cell line: P-glycoprotein as a possible target. *Cancer Chemother. Pharm.* **1994**, *34*, 459–464. [[CrossRef](#)]
60. Bendale, Y.; Bendale, V.; Paul, S. Evaluation of cytotoxic activity of platinum nanoparticles against normal and cancer cells and its anticancer potential through induction of apoptosis. *Integr. Med. Res.* **2017**, *6*, 141–148. [[CrossRef](#)]
61. Peña-Morán, O.A.; Villarreal, M.L.; Álvarez-Berber, L.; Meneses-Acosta, A.; Rodríguez-López, V. Cytotoxicity, post-treatment recovery, and selectivity analysis of naturally occurring podophyllotoxins from *Bursera fagaroides* var. *fagaroides* on breast cancer cell lines. *Molecules* **2016**, *21*, 1013. [[CrossRef](#)]
62. Daina, A.; Michielin, O.; Zoete, V. SwissADME: A free web tool to evaluate pharmacokinetics, drug-likeness and medicinal chemistry friendliness of small molecules. *Sci. Rep.* **2017**, *7*, 1–13. [[CrossRef](#)]
63. Discovery Studio Visualizer V 19. Available online: <https://www.3dsbiovia.com/products/collaborative-science/biovia-discovery-studio/visualization-download.php> (accessed on 18 March 2019).
64. Hunter, A.D. ACD/ChemSketch 1.0 (freeware). *Chem. Educ. Today* **1997**, *74*, 905–906. [[CrossRef](#)]
65. Morris, G.M.; Huey, R.; Lindstrom, W.; Sanner, M.F.; Belew, R.K.; Goodsell, D.S.; Olson, A.J. AutoDock4 and AutoDockTools4: Automated docking with selective receptor flexibility. *J. Comput. Chem.* **2009**, *30*, 2785–2791. [[CrossRef](#)]
66. Morris, G.M.; Goodsell, D.S.; Halliday, R.S.; Huey, R.; Hart, W.E.; Belew, R.K.; Olson, A.J. Automated docking using a Lamarckian genetic algorithm and an empirical binding free energy function. *J. Comput. Chem.* **1998**, *19*, 1639–1662. [[CrossRef](#)]
67. Meng, E.C.; Pettersen, E.F.; Couch, G.S.; Huang, C.C.; Ferrin, T.E. Tools for integrated sequence-structure analysis with UCSF Chimera. *BMC Bioinform.* **2006**, *7*, 1–10. [[CrossRef](#)]
68. Wallace, A.C.; Laskowski, R.A.; Thornton, J.M. LIGPLOT: A program to generate schematic diagrams of protein-ligand interactions. *Protein Eng. Des. Sel.* **1995**, *8*, 127–134. [[CrossRef](#)] [[PubMed](#)]

Sample Availability: Samples of the compounds are available from the authors.



© 2020 by the authors. Licensee MDPI, Basel, Switzerland. This article is an open access article distributed under the terms and conditions of the Creative Commons Attribution (CC BY) license (<http://creativecommons.org/licenses/by/4.0/>).